Heliostat with Automatic Shape Adjustment for High Concentration Throughout the Day

Roger Angel, Nick Didato and Matt Rademacher

Steward Observatory University of Arizona, USA

Abstract. We describe a heliostat which will realize the maximum possible concentration and minimum spillage, by forming an image of the solar disc throughout the day. It uses no drive motors or controls except those needed for dual-axis tracking. The reflector shape is toroidal, with tangential and radial curvature amplitudes and orientations depending on the angle and plane of incidence of the sunlight. We use a “target-axis“ mount, with its first axis pointed in the direction of sunlight reflected to the receiver. The angle of the perpendicular “cross-axis“ is naturally synchronized with the changing angle of the sunlight, so that the required shape change can be obtained simply, using a mechanism coupled directly to the cross-axis drive. A preferred target-axis heliostat design has a rectangular reflector oriented at 45° to the cross-axis and plane of incidence. Shape changes throughout the day are obtained simply by twisting the reflector support frame. Diagonal back struts do this by moving the corners up or down, via mechanical links to the cross-axis motor drive. A specific design using a single, toroidally-bent 8 m^2 glass sheet has been modeled and is now being built at the University of Arizona. A 240 m circular field of 2,064 such heliostats would yield concentrations of between 1,080 to 1,840 suns averaged over a 6.2 m^2 cylindrical receiver, for solar elevations from 20° to 60°. Such high concentrations will enable both higher efficiency conversion of solar to electrical energy and a broader range of thermal uses, including direct production of hydrogen from water.

Keywords: Heliostat, Target-Axis, Disc Image, Automatic Shape Adjustment, High Concentration

Introduction

Over the years CSP has seen progressively increased solar concentration and working temperature, to increase the efficiency of conversion of solar to electrical energy. Early on, trough systems focused sunlight into a line with concentration up to 200 suns, heating oil to ~ 400°C and transfering heat over large distances. CSP systems for electrical generation have now largely transitioned to using heliostats to focus in two dimensions onto a receiver at concentrations of ~ 500x, with molten salt as a transfer and storage medium, and temperatures up to 550°C. Next generation systems are aiming at still higher temperatures. Ongoing tests by Mills et al at the NSTTF with a falling particle cavity receiver have demonstrated that sunlight concentration of 1000 suns can yield receiver outlet temperature of up to 800°C, with 90% of concentrated sunlight energy converted into heat [1]. This temperature can be exploited in thermal-to-electricity conversion at increased efficiency, for example by use of Brayton power cycles with supercritical carbon dioxide (sCO_2). These have the potential to increase efficiency to above 45% for 700°C input temperature, as modeled by Carlson [2]. Another model by Trevisan [3] gives 50% for 660°C input temperature, and 55% for 870°C. These efficiencies are higher than the maximum realized for CSP using a parabolic dish collector. Stirling systems reached 32% with an absorber temperature of 850°C, at a concentration ratio of 1,300 [4].

Even higher temperatures are desirable to obtain still higher Carnot efficiency in conversion of thermal to nechanical energy, and also for other high temperature uses. For example,

direct production of hydrogen can be achieved by solar-thermal redox-based water splitting cycles at a temperature of 1,500°C [5].

Background, Previous Adjustable Shape Heliostats

The highest temperatures require the highest sunlight concentrations. These are realized in a central receiver system where each heliostat in the field forms a solar disc image, centered on the receiver. This high concentration is achieved with minimal spillage loss.

The shape required for a heliostat reflecting surface to focus an image of the sun is a concave toroid, with specific orientation and curvatures chosen according to the relative orientation of the sun, the heliostat and the receiver. The two different radii of curvature in the tangential plane, R_T, and perpendicular sagittal plane R_S are derived using the Coddington equations [6]:

$$R_T = R / \cos(AOI) \quad (1)$$
$$R_S = R. \cos(AOI)$$

where AOI is the angle of incidence of sunlight, and the radius of curvature, R, is chosen to be twice the distance from the mirror center to the receiver. The toroidal surface must be oriented so that the direction of the greater radius, R_T lies in the plane of reflection containing the incident and reflected rays. The required two radii of curvature and the orientation change throughout the day and year, as the reflection geometry changes. Figure 1 shows examples of different toroidal reflector shapes required.

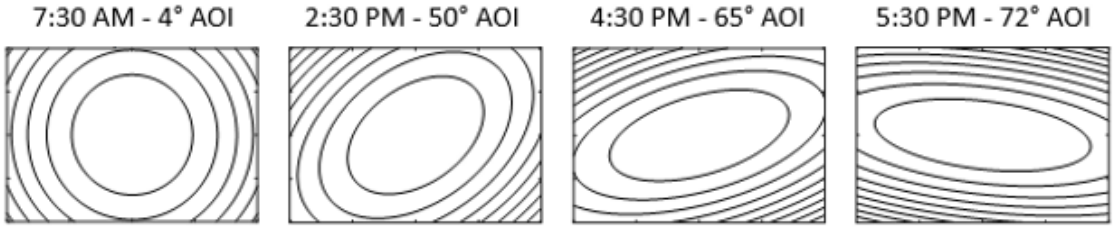

FIGURE 1. Example of the shape changes needed through the day for a focusing heliostat.

An ajustable shape heliostat as shown in Figure 2 was built by Angel et al [7]. It uses an alt-azimuth mount with a single-sheet hexagonal glass mirror 1.8 m^2 in area. The glass was bent to the toroidal shape for 45° AOI and 40 m focal length and attached to a flat hexagonal frame. Six radial back struts extend from a back node on a central, normal strut out to the corners of a hexagonal reflector, as shown in Figure 2, together forming a stiff spaceframe support for the reflector. The shape changes needed to match the different toroidal shapes over a range of angles of incidence are made using three linear actuators at the back node, as shown in Figure 2b. The radial struts are joined in pairs, and connected to the three electrically driven actuators under computer control. Moving an actuator in or out pulls or pushes on the connected diagonally opposite corners, causing them to move up or down together. All the different shapes may be obtained by setting correctly the three actuator strokes. This invention, shown in Figure 2, combines stiffness and the accurate changes in toroidal shape needed to form disc images of the sun, over a wide range of angle of incidence. However, it is complex and expensive

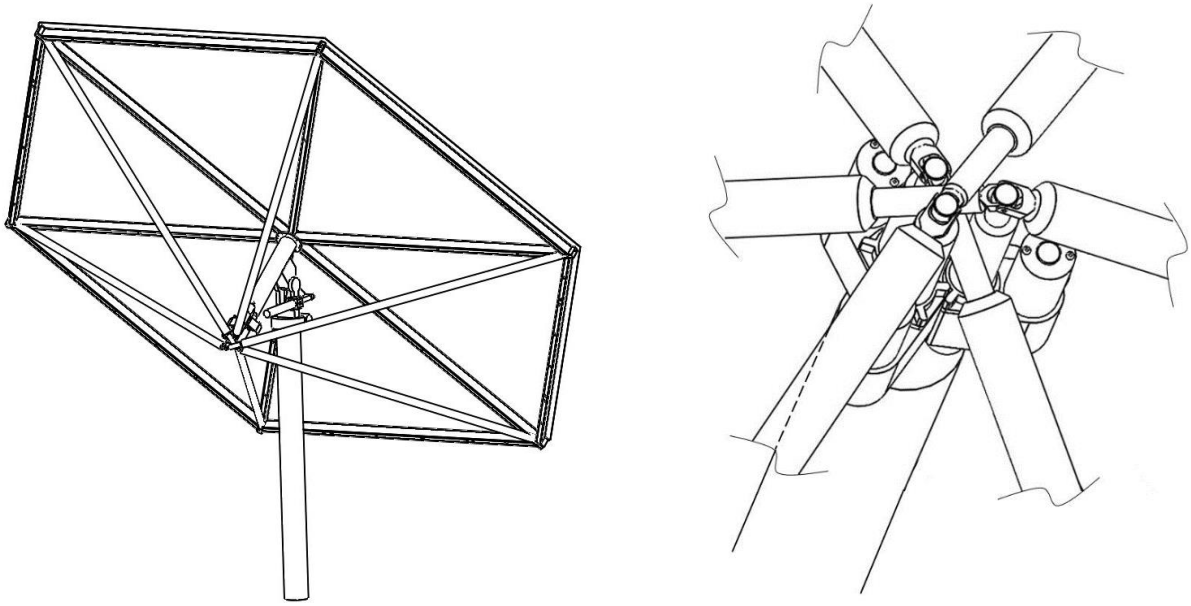

. **FIGURE 2. (a)** Alt-az mounted focusing heliostat with 6 radial and one central axial back strut (b) 3 linear actuators at the back node, coupled to the radial struts

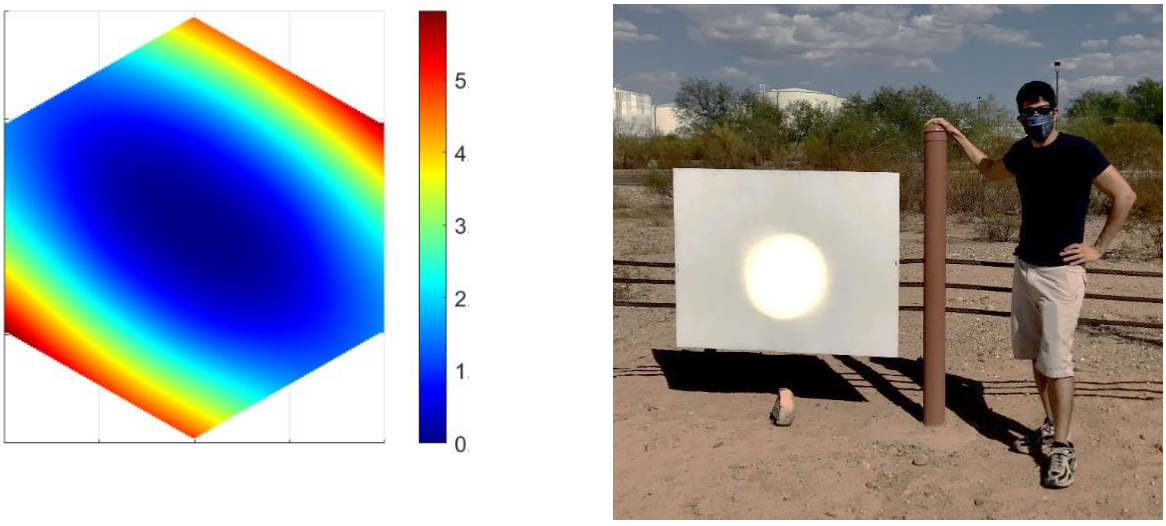

FIGURE 3. (a) surface measurement of the reflector shape actuated for 62° AOI from its base shape for 45° AOI and 40 m focal length (b) image of the solar disc at 62° AOI.

Actuation to obtain the required toroidal shapes may be simplified by using a dual axis mount is of the “target-axis“ type [8]. This has its first axis pointed along the direction of sunlight reflected to the receiver, rather than being vertical as in the conventional alt-azimuth mount used above (Figure 2). The second axis is perpendicular to the first, and the reflector surface is set tangent to it. This configuration has been used previously for shape-adjustable heliostats, taking advantage of the fact that the plane of incidence is fixed in rotation with respect to the reflector, and thus the radial and tangential directions for the toroid are also fixed. The required shape actuation needs then to change only the amplitude of the tangential and radial radii, not their orientation. One such heliostat has been described by Gallar [9], in which the reflecting surface uses many small reflecting segments, oriented by a system of cams and two drive motors. A different approach to changing the curvatures is described by Lehmann et al. [10], in which the reflecting

surface is configured to bend by passive means as the heliostat is rotated to track the sun. In practice, neither of the above two inventions have been adopted for commercial use. A common difficulty is that the provisions made for changing shape reduce stiffness and strength, while commercial heliostats must be very robust so they can both operate in wind and survive very high wind gusts up to 90 mph in stowed position.

Spaceframe heliostat with mechanically coupled shape change

Our new approach uses a stiff, actuated spaceframe heliostat reflector, like that of our earlier system, but now placed on a target axis mount. The shape changes, which now depend only on the cross axis angle (angle of incidence) are obtained simply by mechanical coupling to the cross-axis drive motor, with no need for additional actuators or computer controls. Figure 4a shows an overview of the design. The reflector is rectangular and is oriented at 45° to the cross axis and plane of incidence and reflection, so that the changes in shape required through the day can be obtained simply by twisting the frame. As before, back struts connect the frame corners to central back nodes, as shown in Figure 4b. The two central struts at these nodes are moved axially by mechanical links to the cross-axis motor drive, in order to be in synchronization with the changing angle of incidence. The sagittal axis of bending is aligned to the cross axis of the mount, and one pair of struts from a back node out to the corners is closely aligned to the cross axis. By extending or retracting the central axial strut to this back node, the corners are moved up or down to decrease or increase the sagittal radius. Similarly, the tangential radius is adjusted by a second axial strut.

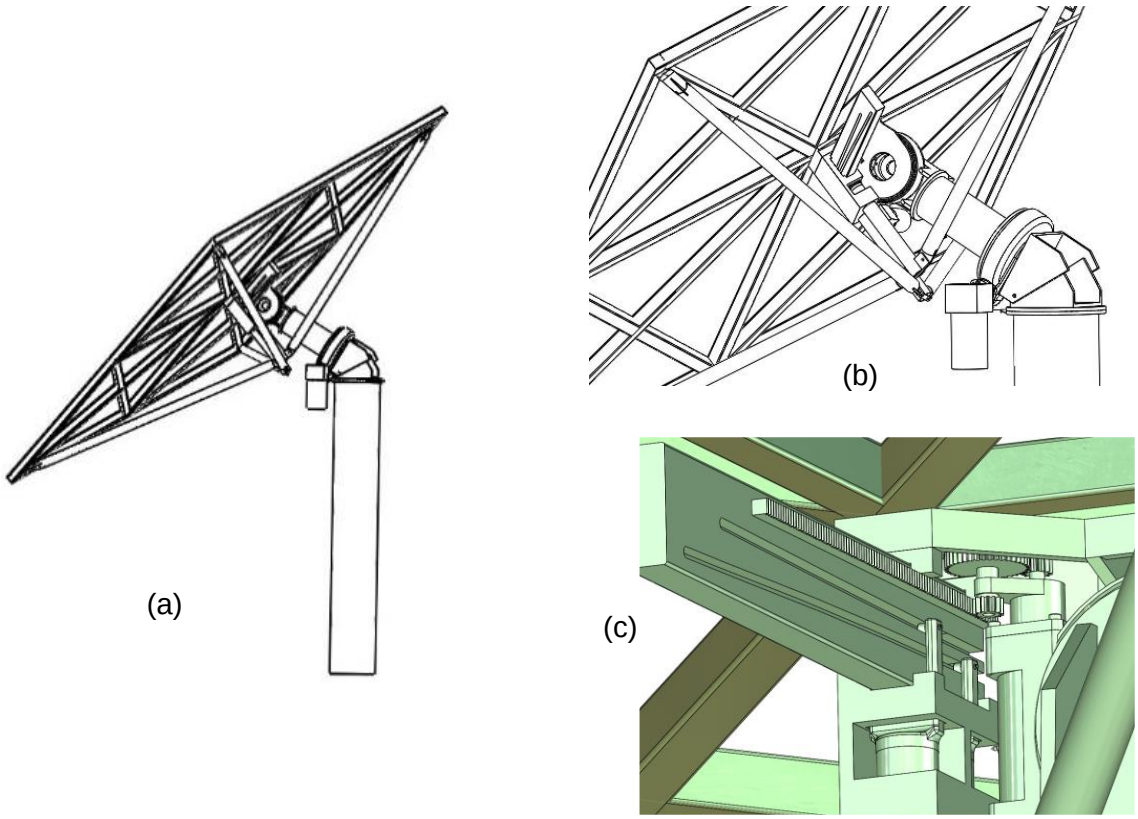

Figure 4. (a) Target-axis mounted heliostat (b) Detail showing of the reflector frame, the target and cross-axis drives, and four corner struts (c) Rack and pinion detail

A detail of the coupled to the cross-axis drive is shown in Figure 4c . A rack moved by a pinion to the cross axis motor has curved grooves machined-in on either side. Wheels in these grooves extend or retract the lower ends of the axial struts.

Performance of a model using a single sheet glass reflector

Here we describe the expected field performance of a heliostat design, modeled using finite element analysis and ray tracing. The reflector is a single flat rectangular sheet of ~~back-silvered glass in~~ the largest size convenient for container shipment, 2.4 x 3.3 m x 3.2 mm thick. The glass is first bent to the toroidal shape needed to focus collimated light at 45° angle of incidence (AOI) to the desired focal distance, Figure 5(c), and then bonded as shown in Figure 5(a) to the support frame set with the actuator struts in the nominal mid-position, (zero push or pull on the corners). A map of this initial surface setting for focal length 120 m is shown in Figure 5(c), with contours at 1 mm spaceing. Figure 5(b) shows the result of strut bending modeled to best match the symmetric shape needed for 0° AOI, and Fig 5d for 60° AOI. The bending shape errors from the model, which includes gravity loading, are less than 0.8 mrad rms.

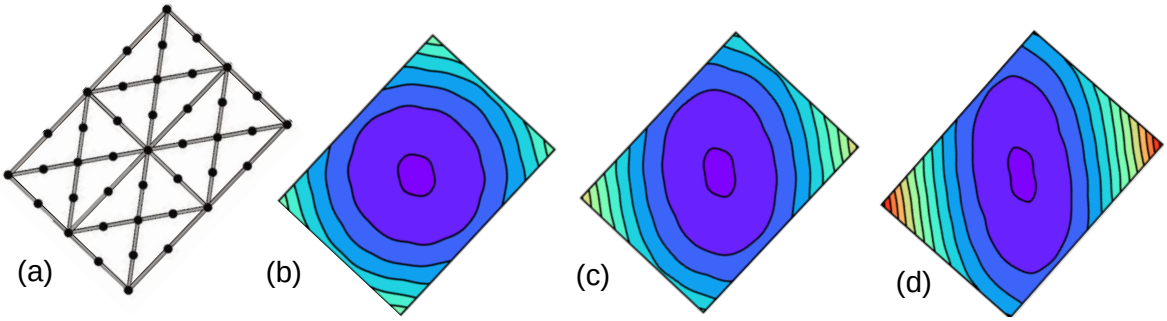

Figure 5. Finite element model of reflector shapes (a) Reflector frame and pattern of 41 attachment pads (b) contours of surface bent for 0° AOI (c) shape as attached to the frame with no actuation, for 45° AOI. (d)) contours of surface bent for 60° AOI

The modeled surfaces of Figure 5 were then loaded into Zemax, and the images formed at 120 m calculated for solar input (top hat source, 30 arcminute diameter. The resulting images are shown in Fig 6, on a 2 m square screen. The upper images are formed with the shape fixed for 45° AOI, the lower two after shape actuation from the finite element model for 0° and 60° AOI, The ensquared energy for all three cases after shape actuation is 89% into a 1 m x 1 m square, and > 99% into a 1.4 m x 1.4 m square. In a joint project now started with Randy Brost of Sandia National Lab, a heliostat as described above is to be built at the University of Arizona and performance chatacterized at the NSTTF.

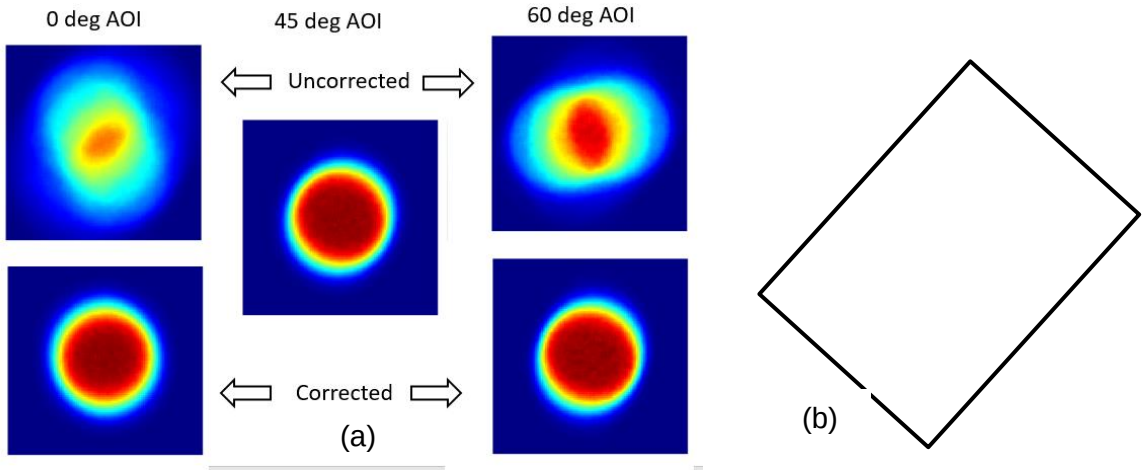

Figure 6. (a) Solar disc images for the reflector shapes of Fig. 5 (b) reflector to same scale.

Example of a 360° Field Using 2,064 Adjustable Shape Heliostats

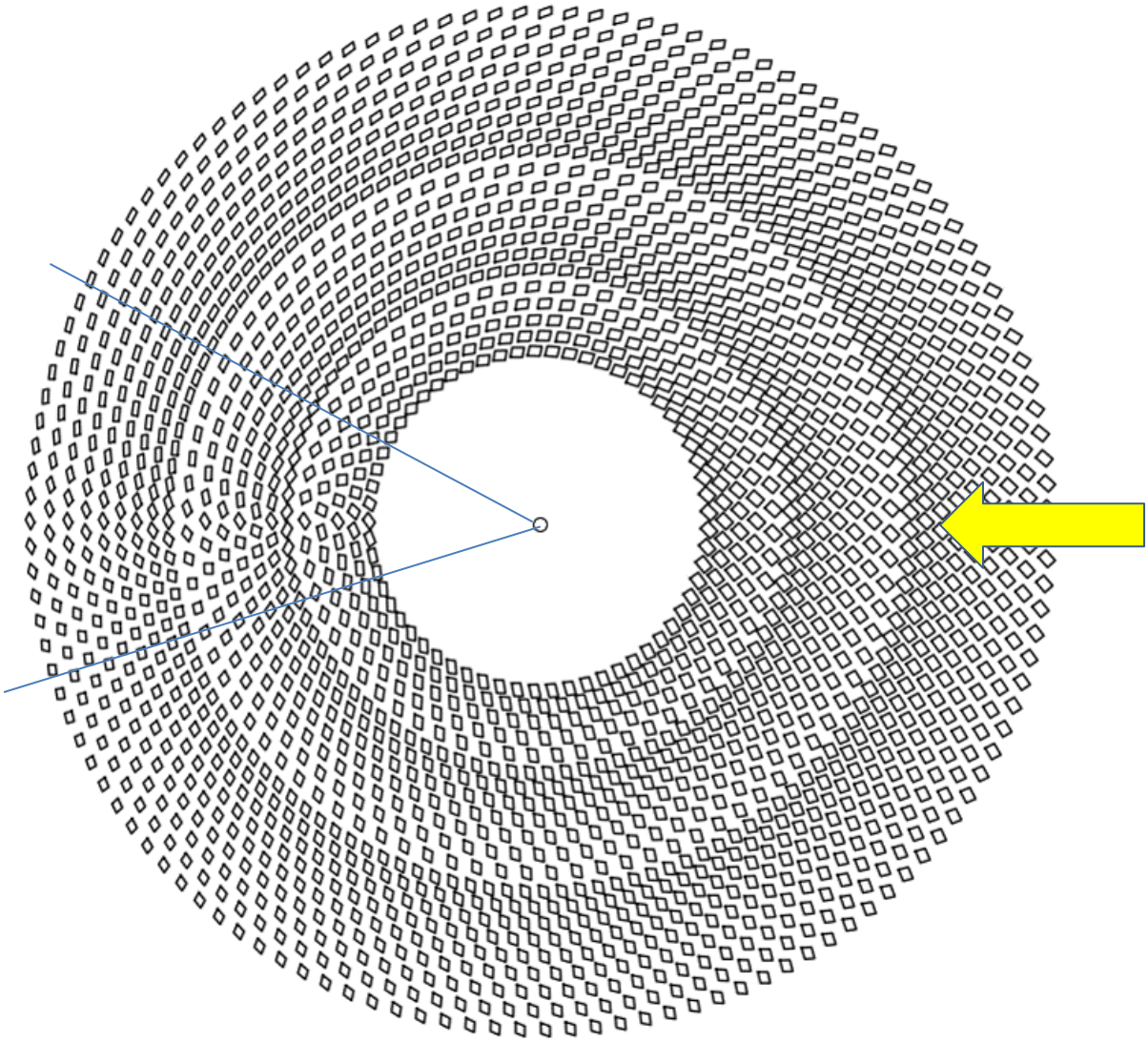

Figure 7. Field of 2,064 heliostats extending from 40 m to 120 m in radius

To obtain the highest receiver temperatures, heliostats need to be arranged in a densely packed field as well as each one having good concentration from disc imaging. To be sure that the unusual 45° orientation of our rectangular reflectors is consistent with dense packing, we have modeled, as an example, a full 360° annular field with 2,064 of the reflectors of the type described above. Figure 7 shows plan view, with the heliostats oriented to reflect sunlight from 40°elevation to a 50 m high central receiver. The field extends in radius from 40 m to 120, and has a total reflector area of 16,600 m^2, 39% of the annular ground area of 40,200 m^2.

Bending stress in the glass reflectors is acceptable, even for the most steeply curved reflectors on the inner diameter at distance 40 m from the receiver tower. The maximum curvature is for an angle of incidence of 60°, when their sagittal radius of curvature must be 64 m and tangential 240 m. Finite element modeling shows that the largest tensile stresses induced by such bending of the originally flat glass sheet is less than < 500 psi. This is a safe level, especially because the front side of the glass, which

must survive stresses from hail impact, is placed in compression by being bent into a concave shape.

The outer heliostats at 120 m radius, whose slant range to the receiver is 130 m, yield solar disc images of nominally 1.08 m in diameter. To determine the optimum size of the cylindrical receiver, we assume a tracking accuracy ≤ 0.5 mrad rms, and, based on the ray tracing scattering model above, we expect that losses averaged over the full field, will then be less than 10% for a cylindrical receiver with height and diameter both of 1.4 m. The surface area is 6.2 m^2, and the ratio of total mirror to receiver area is 2,680.

The actual concentration is reduced by cosine and reflection losses, and in addition by adjacent heliostats which can shadow the incoming sunlight and block some reflected light. These effects were explored by modeling the full field geometry for solar elevations of 20°, 40° and 60°. As an example, the 45° segment of the annular field marked in Figure 7, opposite the sun at 40° elevation, is shown in Figure 8 as seen from the viewpoint of both the sun, Figure 8(a), and the receiver, Figure 8(b). As can be seen, both the shadowing of incoming sunlight and the blocking of light reflected to the receiver by neighboring heliostats are small, amounting to a few percent each. The combination of both losses amounts on average to less than 10% at this location. For heliostats at other locations around the full 360° field, and for solar elevations of both 40° and 60°, these losses are generally even less. At 20° solar elevation the blocking remains very low but shadowing is significant, as is inevitable given long shadows cast by a low sun.

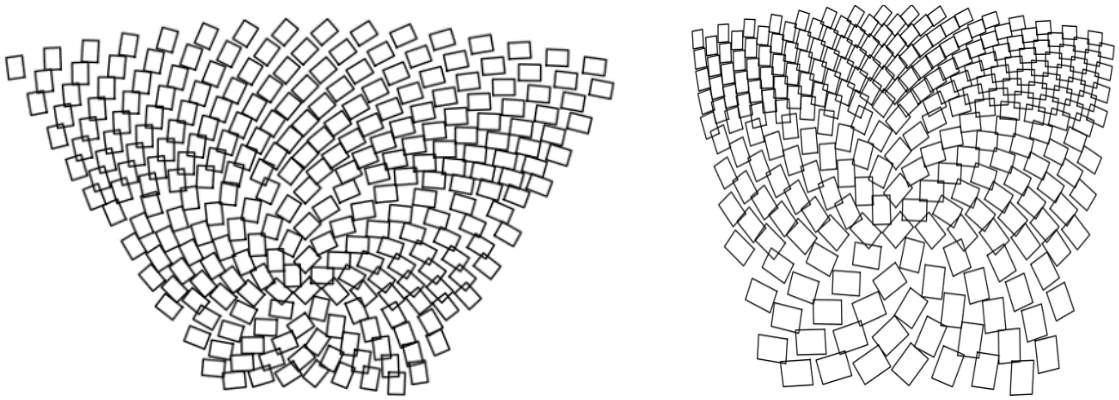

Figure 8. 45° field segment as seen from (a) the sun, and (b) from the receiver

The overall performance of this collection field derived from the above model is summarized in Table 1. Here, to obtain the concentration, we have assumed in addition to the shadowing and blocking a spillage of 10%, based on the performance of the adjustable heliostat given above, and a reflectivity of 90% for the back-silvered mirrors. We find that the sunlight concentration averaged over the cylindrical receiver remains above 1000 suns for all elevations above 20°, peaking at 1,840 x for 60° elevation. Thus given 1 kW/m^2 DNI, the power delivered to the receiver ranges from 8.4 MW at 20° elevation to 11.4 MW at 60°.

Table 1. Characteristics modeled for the 240 m diameter field of Figure 7

Solar elevation	20°	40°	60°
Projected ground area	13,750 m^2	25,840 m^2	34,810 m^2
Area reflected to receiver	8,250 m^2	13,380 m^2	14,080 m^2
Average concentration	1,080	1,760	1,840
Power for 1 kW/m^2 DNI	8.2 MW	10.9 MW	11.4 MW

Conclusion

The above collector is simply one example of how actively focused heliostats could be configured, in this case to obtain very high concentration and temperature for a central external receiver. Other geometries, for example using cavity receivers and/or or secondary reflectors, could also be improved with active, disc-imaging heliostats of this type. The next steps we are taking are to build and test a prototype, and to use the results as a basis for further modeling and cost analysis. This technology could be key in evolving CSP to fully and economically exploit the efficient conversion of solar energy into heat at very high temperature, throughout the day.

Acknowledgements

We are grateful to Joel Berkman for developing the Zemax models given in this paper, and to Dr Justin Hyatt for the reflector metrology system. We thank Steward Observatory for financial support.

References

[1] B. Mills, C. Ho, N. Schroeder, R. Shaeffer, H. Laubscher and K. Albrecht, *Review Design Evaluation of a Next-Generation High-Temperature Particle Receiver for Concentrating Solar Thermal Applications,* Energies 2022, https://doi.org/10.3390/en15051657

[2] M. Carlson , B. Middleton, C. Ho *Techno-Economic Comparison Of Solar-Driven Sco2 Brayton Cycles Using Component Cost Models Baselined With Vendor Data And Estimates,* Proc. ASME 2017

[3] S. Trevisan, R Guedez and Bjorn Laumert „ Supercritical Co2 Brayton Power Cycle For Csp With Packed Bed Test Integration And Cost Benchmark Evaluation Proceedings of the ASME 2019 Power Conference 2019

[4] U. Singh and Anil Kumar*, Review on solar Stirling engine: Development and performance,* Thermal Science and Engineering Progress, **8** pp 244-256 2018,

[5] S. Brendelberger, P. Holzemer-Zerhusen, E. Vega Puga, M. Roeb and C. Sattler, *Study of a new receiver-reactor cavity system with multiple mobile redox units for solar thermochemical water splitting*, Solar Energy **235,** pp 118-128, 2022

[6] J. Landgrave, A.Villalobos, C. González, *Simple mathematical representation of toroidal surfaces,* , Proc., SPIE, **6046,** 2006

[7] R. Angel, R. Eads, N. Didato, M. Rademacher, N. Emerson and C. Davila, *Actively Shaped Focusing Heliostat,* SolarPACES, 2020

[8**]** E. Igel and R. Hughes *Optical analysis of solar facility heliostats,* Solar Energy **22** 283-295, 1979,

[9] L. Gallar *Mixed Heliostat Field,* US Patent 0323772A1 ,2015

[10] Lehmann and Allenspac, *Toroidal heliostat*, Patent PCT/AU2012/000382, 2012